Vol 18 No 6, June 2009
1674-1056/2009/18(06)/2464-05
Chinese Physics B
© 2009 Chin. Phys. Soc.
and IOP Publishing Ltd

Experimental verification of Foreman dislocation model*

Zhao Chun-Wang(赵春旺)[a)†], Xing Yong-Ming(邢永明)[a)], and Bai Pu-Cun(白朴存)[b)]

[a)] *College of Science, Inner Mongolia University of Technology, Hohhot* 010051, *China*

[b)] *College of Materials Science and Engineering, Inner Mongolia University of Technology, Hohhot* 010051, *China*

(Received 3 July 2008; revised manuscript received 12 January 2009)

We present a strain analysis of an edge dislocation core, and a detailed discussion of the Foreman dislocation model. In order to examine the model, the quantitative measurement of strain field around an edge dislocation in aluminum is performed, and high-resolution transmission electron microscopy and geometric phase analysis are employed to map the strain field of the edge dislocation core in aluminum. The strain measurements are compared with the Foreman dislocation model, showing that they are in good agreement with each other when $0.7 \leq a \leq 1.5$.

Keywords: dislocation, strain, high-resolution transmission electron microscopy, geometric phase analysis

PACC: 6170J, 8140L, 6116D

1. Introduction

Dislocation plays a very important role in determining the mechanical properties of materials. Research on dislocation is a classical topic in physics and has aroused much scientific interest. There are quite a number of dislocation models, such as the linear elastic theory and the discrete model. The Peierls–Nabarro[1,2] model is one of the most important models, and it has been discussed extensively.[3−5] Foreman *et al*[6] proposed an improved model. In this model, the Peierls–Nabarro dislocation model is extended to a family of edge dislocations of greater widths by introducing the factor a. Foreman believed that $a = 4$ was suitable for bubble raft experiments.

The numerical simulation method has also been used to study the dislocation in bcc iron,[7,8] Al-Cu alloy,[9] etc. Although extensive research has been carried out in this field, there still exist many unresolved problems. For example, a direct measurement to verify any dislocation model has not yet been accomplished, due to a lack of experimental techniques with sufficient displacement sensitivity and spatial resolution. Recently, development in the quantitative method of image analysis has made it possible to measure deformation fields on a nanoscale.[10] The nanomoiré method has been used to measure deformation to 0.1 nm.[11,12] The scanning moiré method[13] is developed and applied to the deformation measurement on a nanometre scale. The digital nanomoiré method[14] is proposed and the displacement measurement sensitivity can reach the pitch of the lattice of a single crystal. High-resolution transmission electron microscopy (HRTEM) has now become a powerful characterization tool for the structural observation of nanometric structure.[15] HRTEM images of the crystalline lattice are recorded and the deformation fields can also be analysed by using the geometric phase analysis (GPA),[16] which has been applied to a variety of systems, such as the Al/Si nanocluster,[17] nanoparticles,[18] low-angle grain boundaries,[19] strain silicon,[20] etc. Here, we present a study of an edge dislocation in aluminum. The strain field of dislocation core region (−2.25 nm∼ +2.25 nm) is mapped and compared with the Foreman dislocation model.

2. Theory

2.1. Displacement and strain of edge dislocation given by the Peierls–Nabarro model

The Peierls–Nabarro dislocation model describes the displacement of an edge dislocation along the x

*Project supported by the National Natural Science Foundation of China (Grant Nos 10862002 and 10562003).
†E-mail: zhaocw@imut.edu.cn

direction as

$$u_x = -\frac{d}{2\pi}\tan^{-1}\frac{2(1-\nu)x}{y}, \tag{1}$$

where d is lattice constant along the x direction. The strain component ε_{xx} can be written as

$$\varepsilon_{xx} = -\frac{d}{\pi}\frac{(1-\nu)y}{4(1-\nu)^2x^2+y^2}. \tag{2}$$

2.2. Displacement and strain of edge dislocation given by the Foreman model

The Foreman dislocation model describes the displacement of an edge dislocation along the x direction as

$$u_x = -\frac{d}{2\pi}\left[\tan^{-1}\frac{2(1-\nu)x}{ay} + (a-1)\frac{2(1-\nu)xy}{4(1-\nu)^2x^2+a^2y^2}\right], \tag{3}$$

where a is a variable factor, while in the Peierls–Nabarro dislocation model $a = 1$. The strain component ε_{xx} can be written as

$$\varepsilon_{xx} = -\frac{d(1-\nu)}{\pi}\frac{4(1-\nu)^2yx^2+(2a^3-a^2)y^3}{[4(1-\nu)^2x^2+a^2y^2]^2}. \tag{4}$$

3. Experimental methods

3.1. Geometric phase analysis

An HRTEM image of a zone axis of a crystal can be thought of as a set of interference fringes corresponding to the atomic planes of specimens. Performing GPA on these interference fringes individually can extract the displacement information. In particular, by using this technique the displacement of lattice fringes with respect to a perfect lattice can be measured as done in a region of undistorted substrate. This method is based on the calculation of the local Fourier components of the lattice fringes. The phase of these local Fourier components, or geometric phase $P_{\mathrm{g}}(\boldsymbol{r})$, is directly related to the component of the displacement field, $\boldsymbol{u}(\boldsymbol{r})$, in the direction of the reciprocal lattice vector $\boldsymbol{g}$ by

$$P_{\mathrm{g}}(\boldsymbol{r}) = -2\pi\boldsymbol{g}\cdot\boldsymbol{u}(\boldsymbol{r}). \tag{5}$$

It is assumed that the displacement field is constant along the propagation direction through the foil and that if there are small variations, they are averaged out. In the latter case, the displacement field is modeled as the projected displacement field averaged over the foil thickness. By measuring two phase images, $P_{\mathrm{g1}}(\boldsymbol{r})$ and $P_{\mathrm{g2}}(\boldsymbol{r})$, a two–dimensional displacement field can be determined to be

$$\boldsymbol{u}(\boldsymbol{r}) = -\frac{1}{2\pi}[P_{\mathrm{g1}}(\boldsymbol{r})\boldsymbol{a}_1 + P_{\mathrm{g2}}(\boldsymbol{r})\boldsymbol{a}_2], \tag{6}$$

where $\boldsymbol{a}_1$ and $\boldsymbol{a}_2$ are the basis vectors for the lattice in real space, which is corresponding to the reciprocal lattice determined by $\boldsymbol{g}_1$ and $\boldsymbol{g}_2$. Expression (6) can be written in the matrix form

$$\begin{pmatrix} u_x \\ u_y \end{pmatrix} = -\frac{1}{2\pi}\begin{pmatrix} a_{1x} & a_{2x} \\ a_{1y} & a_{2y} \end{pmatrix}\begin{pmatrix} P_{\mathrm{g1}} \\ P_{\mathrm{g2}} \end{pmatrix}. \tag{7}$$

Plane strain can be expressed as

$$\begin{aligned} \varepsilon_{xx} &= \frac{\partial u_x}{\partial x}, \\ \varepsilon_{yy} &= \frac{\partial u_y}{\partial y}, \\ \varepsilon_{xy} &= \frac{1}{2}\left(\frac{\partial u_x}{\partial y} + \frac{\partial u_y}{\partial x}\right). \end{aligned} \tag{8}$$

3.2. Electron microscopy

The experimental material was aluminum, Poisson's ratio $\nu = 0.347$, lattice constant $d_{111} = 0.234$ nm. A transmission electron microscopy (TEM) sample of aluminum was prepared for cross sectional imaging along the $[\bar{1}10]$ direction by using standard techniques involving mechanical grinding followed by ion milling. An HRTEM experiment was performed by using a JEM-2010 transmission electron microscopy at 200 kV. Images were recorded on a Gatan 1 k × 1 k slow scan CCD camera and processed by using the software GPA phase, developed by the Gatan Digital Micrograph environment.

4. Results and discussion

An HRTEM image of an edge dislocation is shown in Fig.1(a). The $(\bar{1}\bar{1}1)$ spot in the Fourier transform of the image in Fig.1(b) was chosen for analysis. A mask was placed around the spot to isolate it and the geometric phase was calculated. The phase is nearly constant in the area away from the dislocation core that was used as a reference. The phase can be calculated as shown in Fig.1(c). The x-axis was chosen to be parallel to the $\boldsymbol{g}_{11\bar{1}}$ orientation, and the y-axis in the perpendicular direction. The strain component ε_{xx} can be determined from expressions (7) and (8).

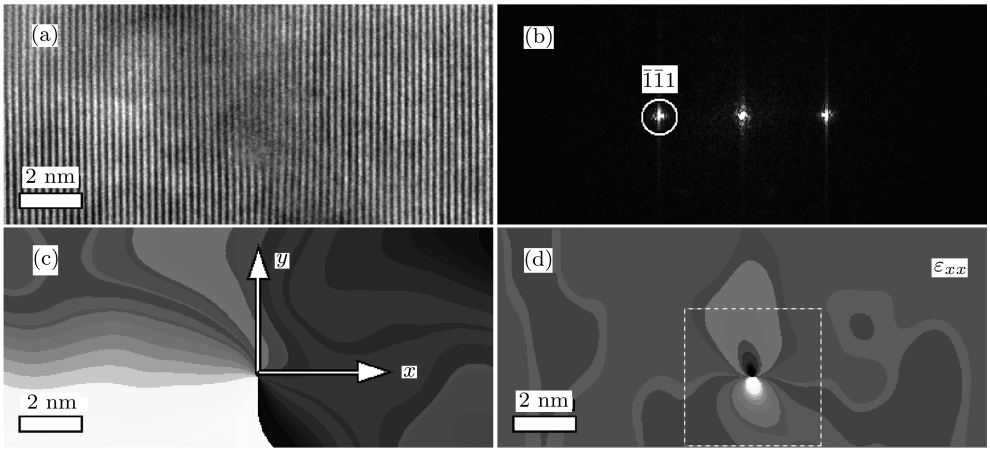


Fig.1. Geometric phase analysis of edge dislocation, where panel (a) shows high-resolution electron microscopy image, panel (b) exhibits Fourier transform of image, with spot analyzed circled, panel (c) displays geometric phase image, and panel (d) presents strain image.

The result is shown in Fig.1(d). There exists a convergence region of strain around the edge dislocation core. The largest values of strain occur in an immediate core region. We can see that the strain becomes increasingly smaller as we move away from the dislocation core.

In order to quantitatively analyse the results in the region of dislocation core, the boxed regions in Fig.1(d) are magnified as shown in Fig.2(a). The size of the boxed region is 4.5 nm × 4.5 nm. In the region of the extra half-plane ($y > 0$), the strains are negative and compressive, and on the other side the lattice is in expansion. It is evident that the strain map is shaped into a figure-eight around the dislocation core. Different values of the dislocation strain component ε_{xx} corresponding to different values of factor a are mapped and shown in Figs.2(b)–2(o). There is no obvious agreement between the model and the immediate core region. The factor a determines the dislocation width. When $a < 0.7$, the strain maps are butterfly shaped (see Figs.2(b)–2(e)). When $a \geq 0.7$, the strain maps become figure-eight shaped (see Figs.2(f)–2(o)). The larger the value of factor a is, the wider the dislocation width will be. Thus, the model is not suitable for the dislocation core for all values of a.

To analyse the degree of agreement between experimental and theoretical results in more detail, the experimental strain component, ε_{xx}, was subtracted from the theoretical strain field. The strain differences are shown in Fig.3. The statistical data on the differences between the experimental and theoretical values of strain component ε_{xx} are shown in Table 1. It can be seen that the differences between experimental and theoretical results are different for different values of factor a. The differences between experimental and theoretical results are smaller when $0.7 \leq a \leq 1.5$ (The means are about 0.00033. The standard deviations are about 0.012), while the differences between experimental and theoretical results are greater when $1.5 < a$ or $a < 0.7$ (The means are greater than 0.00033. The standard deviations are greater than 0.012). Therefore, we consider the Foreman dislocation model to be an appropriate dislocation model when $0.7 \leq a \leq 1.5$.

Table 1. Statistical information on difference between experimental and theoretical values for the strain component ε_{xx}.

a	mean	standard deviation	a	mean	standard deviation
0.3	0.0003413	0.11	1.0	0.0003308	0.012
0.4	0.0003390	0.048	1.5	0.0003347	0.012
0.5	0.0003367	0.023	2.0	0.0003450	0.013
0.6	0.0003351	0.014	3.0	0.0003647	0.016
0.7	0.0003330	0.012	4.0	0.0003799	0.020
0.8	0.0003317	0.012	7.0	0.0004054	0.025
0.9	0.0003310	0.012	10.0	0.0004175	0.028

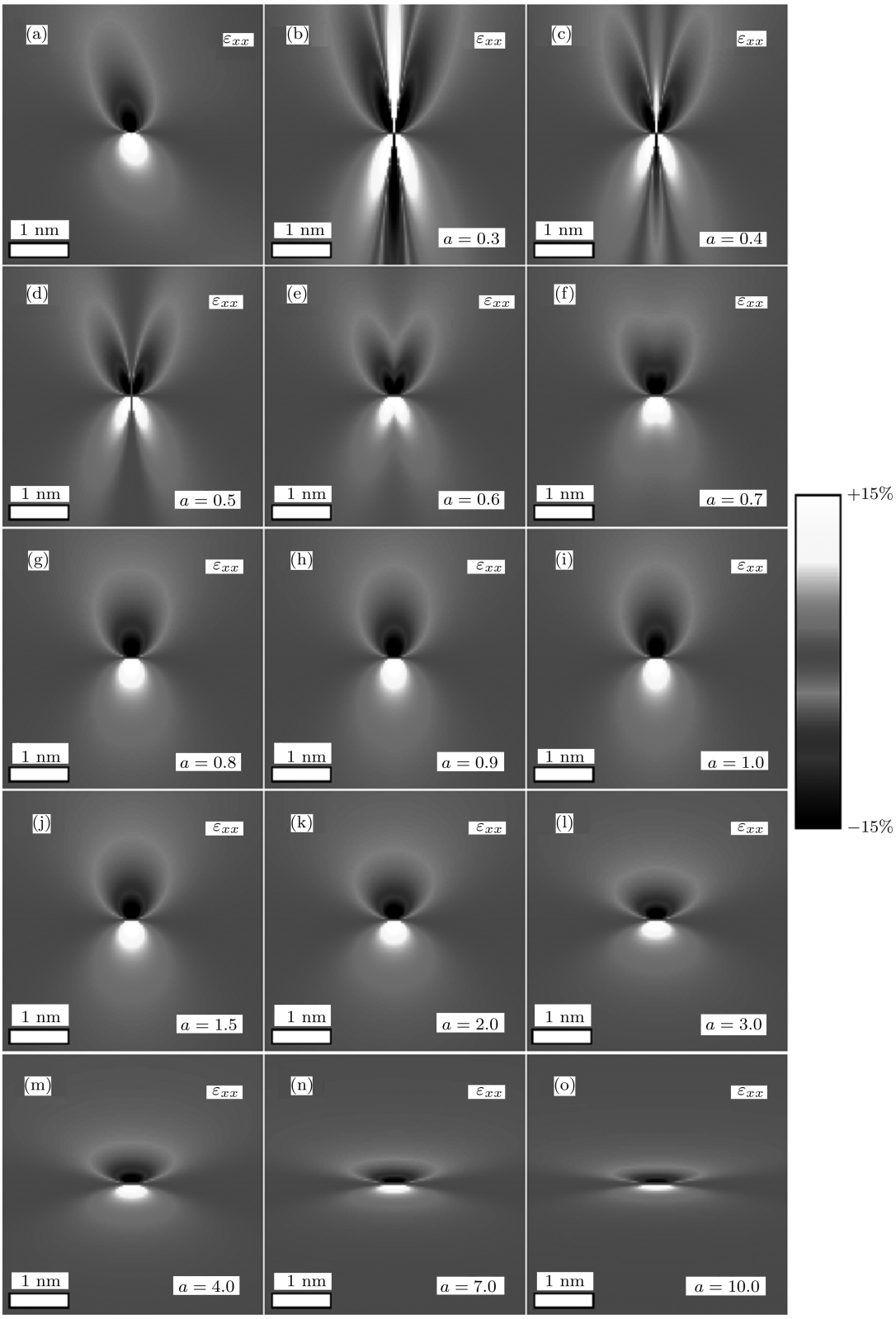


Fig.2. Experimental strain map and theoretical strain map corresponding to different values of factor a for the Foreman model, where panel (a) shows experimental strain map, panels (b)–(o) display theoretical strain maps corresponding to different values of factor a for the Foreman model.

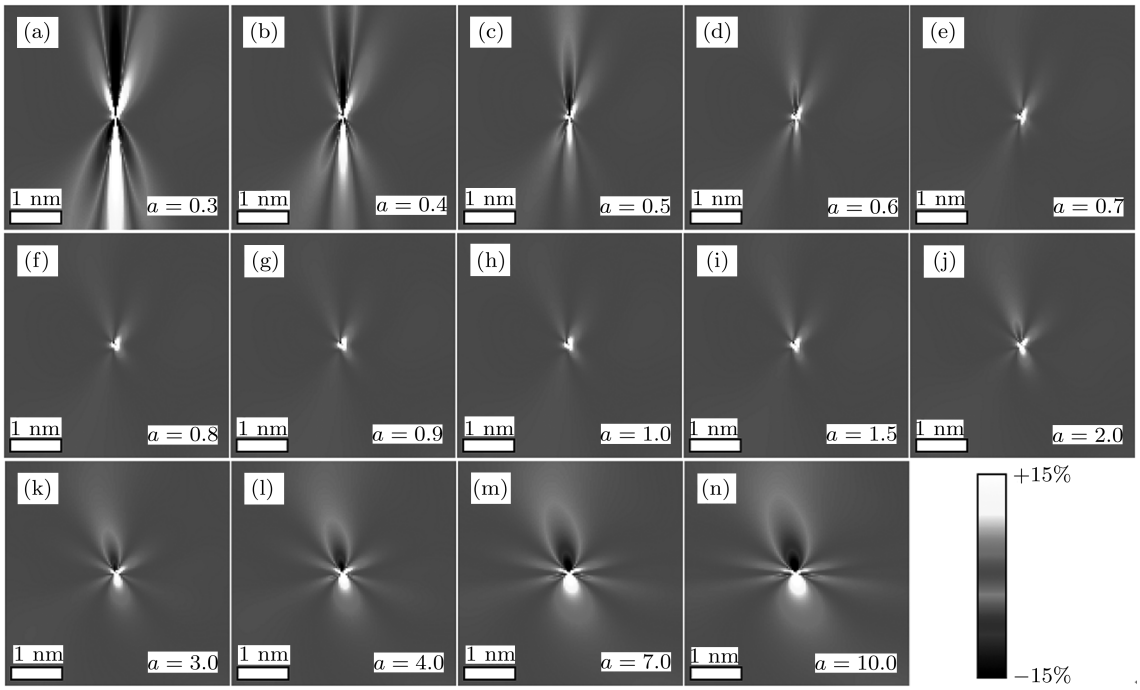


Fig.3. Strain differences between experimental strain field and theoretical strain field at different values of factor a for the Foreman model.

5. Conclusions

The Foreman dislocation model is discussed in detail. A direct quantitative measurement of the strain field around an edge dislocation core in aluminum is achieved through a combination of high-resolution transmission electron microscopy and geometric phase analysis. The experimental measurements are compared with theoretical calculations, and it was found that the Foreman dislocation model can describe the strain field of the dislocation core for $0.7 \leq a \leq 1.5$.

References

[1] Peierls R E 1940 *Proc. Phys. Soc. Lond.* **52** 34
[2] Nabarro F R N 1947 *Proc. Phys. Soc. Lond.* **59** 256
[3] Hansen L B, Stokbro K, Lundqvist B I, Jacobsen K W and Deaven D M 1995 *Phys. Rev. Lett.* **75** 4444
[4] Yao Y G, Wang T C and Wang C Y 1999 *Phys. Rev.* B **59** 8232
[5] Wang S F 2005 *Chin. Phys.* **14** 2575
[6] Foreman A J, Jaswon M A and Wood J K 1951 *Proc. Phys. Soc. Lond.* A **64** 156
[7] Chen L Q, Yu T, Wang C Y and Qiu Z C 2008 *Acta Phys. Sin.* **57** 443 (in Chinese)
[8] Chen L Q, Wang C Y and Yu T 2008 *Chin. Phys.* B **17** 662
[9] Jiang H F, Zhang Q C, Chen X D, Fan Z C, Chen Z J and Wu X P 2007 *Acta. Phys. Sin.* **56** 3388 (in Chinese)
[10] Kret S, Ruterana P, Rosenauer A and Gerthsen D 2001 *Phys. Status. Solidi* B **227** 247
[11] Dai F L and Xing Y M 1999 *Acta Mech. Sin.* **15** 283
[12] Xing Y M, Dai F L and Yang W 2000 *Sci. Chin.* A **43** 963
[13] Xie H M, Kishimoto S, Asundi A, Boay C G, Shinya N, Yu J and Ngoi B K A 2000 *Nanotechnology* **11** 24
[14] Xie H M, Liu Z W, Fang D N, Dai F L, Gao H J and Zhao Y P 2004 *Meas. Sci. Technol.* **15** 1716
[15] Schäublin R 2006 *Microsc. Res. Techniq.* **69** 305
[16] Zhao C W, Xing Y M, Zhou C E and Bai P C 2008 *Acta Mater.* **56** 2570
[17] Liu Z W, Xie H M, Fang D N, Dai F L, Xue Q K, Liu H and Jia J F 2005 *Appl. Phys. Lett.* **87** 201908
[18] Johnson C L, Snoeck E, Ezcurdia M, Rodríguez-González B, Pastoriza-Santos I, Liz-Marzán L M and Hÿtch M J 2008 *Nature Mater.* **7** 120
[19] Zhao C W, Xing Y M, Bai P C, Hou J F and Dai X J 2008 *Physica* B **403** 1838
[20] Hüe F, Hÿtch M, Bender H , Houdellier F and Claverie A 2008 *Phys. Rev. Lett.* **100** 156602